



Positive-Negative Array-Element Based Single-Antenna Full-Duplex Self-Interference Mitigation

Wenchi Cheng*, Jianyu Wang, and Hailin Zhang

State Key Laboratory of Integrated Services Networks, Xidian University, Xi'an, 710000, China

Abstract

Full-duplex (FD), where the terminal transmits and receives signals simultaneously using the same frequency-band and time-slots, has been treated as one of the potential candidate techniques to enhance the spectrum of future wireless communications. However, one of critical problems in wireless FD communications is how to efficiently mitigate the self-interference (SI) while achieving the maximum spectrum efficiency. In this paper, we develop novel positive-negative array-element based SI mitigation scheme for wireless FD communications. In particular, we formulate the system model for positive-negative array-element based SI mitigation scheme. Then, based on the system model, we analyze the performance of the SI mitigation scheme. Simulation results verify our theoretical analyses and show that our developed SI mitigation schemes can significantly reduce SI for wireless FD communications.

1 Introduction

By enabling simultaneous transmission and reception using the same frequency-band and time-slots, full-duplex (FD) can significantly boost the spectrum efficiency for wireless communications. It has become one of the potential candidate techniques for future wireless communications and networks [1]. A number of challenging problems, such as self-interference (SI) cancellation, self-interference adaptive resource allocation, and asynchronous FD coding/decoding, need to be efficiently solved to achieve the exciting double spectrum efficiency for wireless FD communications as compared with the traditional half-duplex communications [2].

Since the SI is much stronger than the received signal from other mobile terminals, it is very difficult to completely cancel SI in wireless FD communications. The types of SI can be classified into two categories: inter-SI, which refers to the interference leaked from the transmitter into the receiver, and intra-SI, which is the interference resulted within the transceiver. The inter-SI can be mitigated using multiple antenna resource while the intra-SI can only be reduced using single-antenna based SI cancellation techniques. In recent years, a number of multi-antenna techniques cancellation techniques have been developed to suppress the SI

before it overwhelms the low-noise-amplifier (LNA). For full-duplex MIMO communication systems, the authors of [3] present a two-stage SI mitigation method, which refers to employing the compressed sensing-based SI estimation technique in the first stage to partly reduce the power of SI, and applying a subspace-based algorithm in the second stage to further estimate the coefficient of intended channel as well as further mitigate the residual SI. The authors of [4] placed two transmit antennas at distances d and $d + \lambda$ from the receive antenna, where λ is the wavelength of the carrier, to create a null position and mitigate the inter-SI. In [5], the authors proposed to use passive antenna separation, additional radio frequency (RF) chain, and active digital cancellation to reduce the inter-SI.

However, antenna resource is very important in many kinds of mobile smart products, such as smart phones, smart watches, and smart glasses [6]. Therefore, although the multi-antenna techniques can efficiently mitigate the inter-SI, many researchers are further interested in mitigating the SI using other techniques. There exist works focusing on the electrical balance or CMOS circulator to cancel the intra-SI [7, 8]. In [7], the authors reviewed the challenges of providing high transmit-to-receive isolation over wide bandwidths with electrical balance in hybrid junctions. In [8], the authors developed a new CMOS circulator, which splits the transmit signal into two paths of an exact π phase difference, to suppress the SI. However, these circuit-based transmit-to-receive isolation schemes are sensitive to antenna impedance variation in both the frequency domain and time domain, limiting the isolation bandwidth and requiring dynamic adaptation.

To facilitate the implementation of FD into future wireless communications, both the inter-SI and the intra-SI need to be efficiently canceled without sacrificing the antenna resource. Also, not only the circuit-based transmit-to-receive isolation, but also the digital domain need to be compatible with the single antenna based SI mitigation. With these goals in mind, in this paper we develop a single positive-negative array-element based SI mitigation scheme to mainly reduce the SI. The obtained simulation results verify the theoretical analyses and show that our developed SI mitigation schemes can significantly reduce the intra/inter-SI.

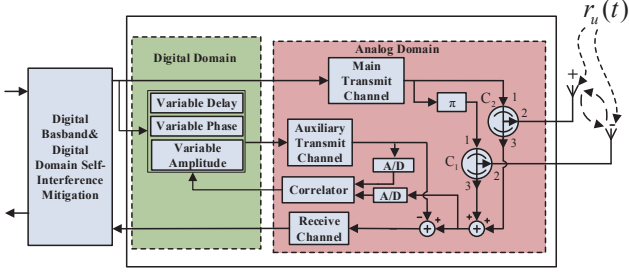


Figure 1. The positive-negative array-element block diagram.

2 System Model

Figure 1 shows the block diagram of positive-negative array-element, where two array-elements have the same amplitude and frequency but a phase difference of π . We assume that the array-element connected to the inverter (denoted by π in Fig. 1) is negative array-element and the other is positive array-element. We refer to this type of a pair of positive and negative array-elements as a positive-negative array-element. Each array-element is connected to one circulator. The transmit signal leaks through the circulators, forming the intra-SI. On the other hand, the positive and negative array-elements cause interferences to each other, forming the inter-SI. Due to the π phase difference, the combination after the two circulators can partially mitigate intra-SI and inter-SI, which guarantees that the partially mitigated SI does not overwhelm the useful received signal. Then, the estimated main part of SI goes through the auxiliary transmit channel and sampled by another A/D. The correlator guarantees that the output of auxiliary transmit channel is equal to the main part of SI. The receive channel will finally get the signal with residual SI (including both intra-SI and small inter-SI), which can be handled in digital-domain. The detailed formulations will be described in the next section.

3 Positive-Negative Array-Element Intra/Inter Self Interference Mitigation

For the positive-negative array-element, we need to mitigate the intra-SI within the array-elements themselves as well as the inter-SI between the positive and negative array-elements. The impulse responses of the main transmit channel corresponding to the positive and negative array-elements, denoted by $I_p(t)$ and $I_n(t)$, respectively, can be given as follows:

$$\begin{cases} I_p(t) = \sum_{l=1}^L a_l(t) e^{j\theta_l(t)} \delta(t - \tau_l); \\ I_n(t) = - \sum_{l=1}^L a_l(t) e^{j\theta_l(t)} \delta(t - \tau_l), \end{cases} \quad (1)$$

where L is the total number of multipath, t is time variable, $a_l(t)$ is the amplitude response corresponding to the l th path, $\theta_l(t)$ is the phase response corresponding to the l th path, and τ_l is the delay corresponding to the l th path. The

transmit signal leaks to the receiver through the circulator. Then, the impulse responses after the circulator, denoted by $I_{c,p}(t)$ and $I_{c,n}(t)$, respectively, for the main channel can be derived as Eq. (2), which is on the top of next page. We denote by $k_{ab}(t)$ and $\tilde{k}_{ab}(t)$ the amplitude attenuations from port a to port b ($ab \in \{12, 13, 23\}$) of the circulator corresponding positive and negative array-element, respectively. $\omega_{ab}(t)$ and $\tilde{\omega}_{ab}(t)$ are the phase-shift from port a to port b caused by the circulator corresponding to positive and negative array-element, respectively. ϵ_{ab} and $\tilde{\epsilon}_{ab}$ represent the delay from port a to port b of the circulator corresponding to positive and negative array-element, respectively. $h_{p,n}(t)$ is the amplitude and phase response of the channel from positive array-element to negative array-element, and $h_{n,p}(t)$ denotes the amplitude and phase response of the channel from negative array-element to positive array-element. $\eta_{p,n}$ and $\eta_{n,p}$ are the delay corresponding to $h_{p,n}(t)$ and $h_{n,p}(t)$, respectively. Thus, the SI mixed signal (including the intra-SI, the inter-SI, and the received useful signal from the other mobile terminals) after the circulator, denoted by $y_p(t)$ and $y_n(t)$, respectively, can be derived as follows:

$$\begin{cases} y_p(t) = x(t) * I_{c,p}(t) \\ \quad \quad \quad + r_u(t) * k_{23}(t) e^{j\omega_{23}(t)} \delta(t - \epsilon_{23}); \\ y_n(t) = x(t) * I_{c,n}(t) \\ \quad \quad \quad + r_u(t) * \tilde{k}_{23}(t) e^{j\tilde{\omega}_{23}(t)} \delta(t - \tilde{\epsilon}_{23}), \end{cases} \quad (3)$$

where $x(t)$ is the local transmit signal and $r_u(t)$ is the received useful signal. As we know, $x(t)$ is known to the local receiver. Based on Eq. (3), the entire received signal before SI mitigation, denoted by $y_i(t)$, can be derived as follows:

$$\begin{aligned} y_i(t) &= y_p(t) + y_n(t) \\ &= \sum_{l=1}^L a_l(\tau_l) e^{j\theta_l(\tau_l)} x(t - \tau_l) * [\alpha_i(t) + \beta_i(t)] \\ &\quad \quad \quad + r_u(t) * \gamma_i(t), \end{aligned} \quad (4)$$

where $\alpha_i(t)$ and $\beta_i(t)$ represent the impulse responses of the combined channel corresponding to the main transmit channel, two circulators, and the adder for intra-SI and inter-SI, respectively. $\gamma_i(t)$ represents the combined impulse response from port 2 to port 3 of two circulators. The expressions for $\alpha_i(t)$, $\beta_i(t)$, and $\gamma_i(t)$ are given in Eq. (5), which is on the next page. Then, the correlator can sample $y_i(t)$ as follows:

$$y_i(m) = y_i(t)|_{t=mT_s}, \quad (6)$$

where T_s is the sampling period. The estimated main part of SI corresponding to the auxiliary transmit channel, denoted by $z(m)$, can be written as follows:

$$z(m) = \sum_{l=1}^L \tilde{a}_l(\tilde{\tau}_l) e^{j\tilde{\theta}_l(\tilde{\tau}_l)} x(mT_s - \tilde{\tau}_l), \quad (7)$$

where $\tilde{a}_l(\tilde{\tau}_l)$ is the amplitude response corresponding to the l th path of the auxiliary transmit channel, $\tilde{\theta}_l(\tilde{\tau}_l)$ is the phase response corresponding to l th path of the auxiliary transmit channel, and $\tilde{\tau}_l$ is the corresponding delay. To remove the main part of intra/inter-SI, we make the crosscorrelation, denoted by $R_i(n)$, for $y_i(m)$ and $z(m)$ as follows:

$$\begin{cases}
I_{c,p}(t) = \underbrace{\sum_{l=1}^L k_{13}(\varepsilon_{13}) a_l(t - \varepsilon_{13}) e^{j[\theta_l(t - \varepsilon_{13}) + \omega_{13}(\varepsilon_{13})]} \delta(t - \tau_l - \varepsilon_{13})}_{\text{intra-SI}} \\
\quad - \underbrace{\sum_{l=1}^L h_{n,p}(\eta_{n,p}) \tilde{k}_{12}(\tilde{\varepsilon}_{12}) k_{23}(\varepsilon_{23}) a_l(t - \varepsilon_{23} - \tilde{\varepsilon}_{12} - \eta_{n,p})}_{\text{inter-SI}} \\
\quad \quad e^{j[\theta_l(t - \varepsilon_{23} - \tilde{\varepsilon}_{12} - \eta_{n,p}) + \tilde{\omega}_{12}(\tilde{\varepsilon}_{12}) + \omega_{23}(\varepsilon_{23})]} \delta(t - \varepsilon_{23} - \tilde{\varepsilon}_{12} - \eta_{n,p} - \tau_l); \\
I_{c,n}(t) = - \underbrace{\sum_{l=1}^L \tilde{k}_{13}(\varepsilon_{13}) a_l(t - \tilde{\varepsilon}_{13}) e^{j[\theta_l(t - \tilde{\varepsilon}_{13}) + \tilde{\omega}_{13}(\tilde{\varepsilon}_{13})]} \delta(t - \tau_l - \tilde{\varepsilon}_{13})}_{\text{intra-SI}} \\
\quad + \underbrace{\sum_{l=1}^L h_{p,n}(\eta_{p,n}) k_{12}(\varepsilon_{12}) \tilde{k}_{23}(\tilde{\varepsilon}_{23}) a_l(t - \tilde{\varepsilon}_{23} - \varepsilon_{12} - \eta_{p,n})}_{\text{inter-SI}} \\
\quad \quad e^{j[\theta_l(t - \tilde{\varepsilon}_{23} - \varepsilon_{12} - \eta_{p,n}) + \omega_{12}(\varepsilon_{12}) + \tilde{\omega}_{23}(\tilde{\varepsilon}_{23})]} \delta(t - \tilde{\varepsilon}_{23} - \varepsilon_{12} - \eta_{p,n} - \tau_l),
\end{cases} \quad (2)$$

$$\begin{cases}
\alpha_i(t) = k_{13}(t) e^{j\omega_{13}(t)} \delta(t - \varepsilon_{13}) - \tilde{k}_{13}(t) e^{j\tilde{\omega}_{13}(t)} \delta(t - \tilde{\varepsilon}_{13}); \\
\beta_i(t) = k_{12}(\varepsilon_{12}) \tilde{k}_{23}(\tilde{\varepsilon}_{23}) h_{p,n}(t - \tilde{\varepsilon}_{23} - \varepsilon_{12}) e^{j[\omega_{12}(\varepsilon_{12}) + \tilde{\omega}_{23}(\tilde{\varepsilon}_{23})]} \delta(t - \tilde{\varepsilon}_{23} - \varepsilon_{12} - \eta_{p,n}) \\
\quad - \tilde{k}_{12}(\tilde{\varepsilon}_{12}) k_{23}(\varepsilon_{23}) h_{n,p}(t - \varepsilon_{23} - \tilde{\varepsilon}_{12}) e^{j[\tilde{\omega}_{12}(\tilde{\varepsilon}_{12}) + \omega_{23}(\varepsilon_{23})]} \delta(t - \varepsilon_{23} - \tilde{\varepsilon}_{12} - \eta_{n,p}); \\
\gamma_i(t) = k_{23}(t) e^{j\omega_{23}(t)} \delta(t - \varepsilon_{23}) + \tilde{k}_{23}(t) e^{j\tilde{\omega}_{23}(t)} \delta(t - \tilde{\varepsilon}_{23}).
\end{cases} \quad (5)$$

$$R_i(n) = \sum_{m=-\infty}^{\infty} [y_i(m) z(m+n)]. \quad (8)$$

Thus, the delay of the main part corresponding to the SI, denoted by n_o , can be obtained through

$$n_o = \arg \max_n R_i(n). \quad (9)$$

Then, we can adaptively adjust the amplitude and phase corresponding to the auxiliary transmit channel to make the correlation coefficient be equal to 1 as follows:

$$\frac{R_i(n)}{\sqrt{\mathbb{E}(y_i^2(m)) \mathbb{E}(z^2(m))}} = 1, \quad (10)$$

where \mathbb{E} denotes the expectation. Then, we can remove the main part of intra/inter-SI and obtain the SI mitigated signal denoted by $y'_i(m)$, for the positive-negative array-element as Eq. (11), which is on the top of next page.

4 Performance Evaluations

In this section, we conduct numerical and simulation experiments to evaluate the performance of our proposed self-interference mitigation schemes for the FD wireless communications. Throughout our simulations, we choose the coaxial circulator (UIY-CC2628A) with the frequency range 2401-2423 MHz and use linear minimum mean square error (LMMSE) criterion to estimate the impulse responses for multiple paths.

Employing our proposed positive-negative array-element based SI mitigation scheme, we make twice simulations to evaluate the deviation between the auxiliary signal and the

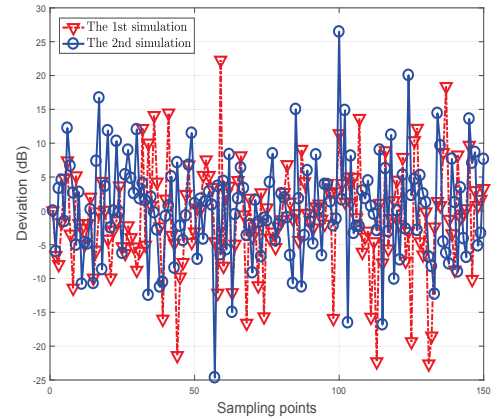


Figure 2. The deviation between the auxiliary signal and the SI signal.

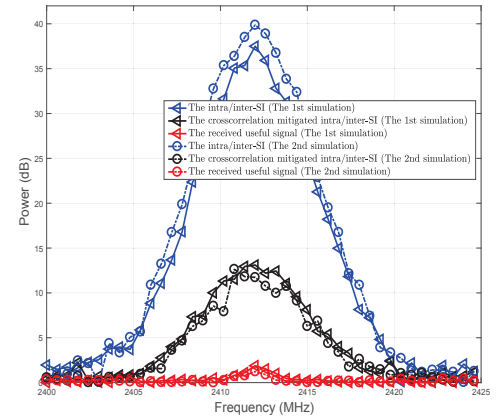


Figure 3. The intra/inter-SI mitigation for one positive-negative array-element using the correlation based scheme.

$$\begin{aligned}
y'_i(m) &= y_i(m) - z(m) \\
&= \sum_{l=1}^L \left(\underbrace{-\tilde{a}_l(\tilde{\tau}_l) e^{j\tilde{\theta}_l(-\tilde{\tau}_l)} x(n_o T_s - \tilde{\tau}_l)}_{\text{the main part of SI}} + a_l(\tau_l) e^{j\theta_l(\tau_l)} \left[k_{13}(\epsilon_{13}) e^{j\omega_{13}(t)} x(mT_s - \epsilon_{13} - \tau_l) - \tilde{k}_{13}(\tilde{\epsilon}_{13}) e^{j\tilde{\omega}_{13}(t)} x(mT_s - \tilde{\epsilon}_{13} - \tau_l) \right. \right. \\
&\quad + k_{12}(\epsilon_{12}) \tilde{k}_{23}(\tilde{\epsilon}_{23}) h_{p,n}(\eta_{p,n}) e^{j[\omega_{12}(\epsilon_{12}) + \tilde{\omega}_{\epsilon_{23}}]} x(mT_s - \tilde{\epsilon}_{23} - \epsilon_{12} - \eta_{p,n} - \tau_l) \\
&\quad \left. \left. - \tilde{k}_{12}(\tilde{\epsilon}_{12}) k_{23}(\epsilon_{23}) h_{n,p}(\eta_{n,p}) e^{j[\tilde{\omega}_{12}(\tilde{\epsilon}_{12}) + \omega_{\epsilon_{23}}]} x(mT_s - \epsilon_{23} - \tilde{\epsilon}_{12} - \eta_{n,p} - \tau_l) \right] \right) \\
&\quad + k_{23} e^{j\omega_{23}(\epsilon_{23})} y_u(mT_s - \epsilon_{23}) + \tilde{k}_{23}(\tilde{\epsilon}_{23}) e^{j\tilde{\omega}_{23}(\tilde{\epsilon}_{23})} r_u(mT_s - \tilde{\epsilon}_{23}).
\end{aligned} \tag{11}$$

SI signal, which is illustrated in Fig. 2. To obtain the estimated main part of the SI, the SI signals are sampled for multiple times. Then, the main part of the SI can be mitigated after the correlation processing. As shown in Fig. 2, most of the deviation points are concentrated in around 10 dB and the maximum deviation is about 27 dB.

Figure 3 shows the performance of SI mitigation within the positive-negative array-element employing our proposed crosscorrelation based scheme. We also make twice simulations to evaluate our proposed SI mitigation method. As illustrated in Fig. 3, after the A/D sampling, the power of intra/inter-SI can be effectively mitigated by crosscorrelation processing. In particular, with the error caused by the fading of channel, the power corresponding to SI is significantly mitigated by about 24-27 dB at the central frequency 2412 MHz.

5 Conclusion

In this paper, we proposed the positive-negative array-element based single-antenna SI mitigation system model for FD wireless communications. Based on the system model, we analyze the performance of our proposed SI mitigation framework. Simulation results verify theoretical analyses and show that our developed self-interference mitigation schemes can significantly reduce the intra/inter-SI without sacrificing the antenna resource. Our developed SI mitigation schemes can be jointly used with the advanced circuit SI mitigation technologies to achieve much high SI attenuation.

6 Acknowledgements

This work was supported in part by the National Natural Science Foundation of China (NO. 61771368) and Young Elite Scientists Sponsorship Program by CAST (2016QN-RC001).

References

[1] X. Zhang, W. Cheng and H. Zhang, "Full-duplex transmission in phy and mac layers for 5G mobile wireless networks," *IEEE Wireless Commu-*

nications, **22**, 5, October 2015, pp. 112–121, doi:10.1109/MWC.2015.7306545.

- [2] D. Guo, D. W. Bliss, S. Rangarajan, and R. Wichman, "In-band full-duplex wireless: Challenges and opportunities," *IEEE Journal on Selected Areas in Communications*, **32**, 9, September 2016, pp. 1637–1652, doi: 10.1109/JSAC.2014.2330193.
- [3] A. Masmoudi and T. Le-Ngoc, "Channel estimation and self-interference cancellation in full-duplex communication systems," *IEEE Transactions on Vehicular Technology*, **66**, 1, January 2017, doi: 10.1109/TVT.2016.2540538.
- [4] J. Choi, M. Jain, K. Srinivasan, P. Levis, and S. Katti, "Achieving single channel, full duplex wireless communication," *16th ACM MOBICOM*, Chicago, Illinois, USA, September 2010, doi: 10.1145/1859995.1859997.
- [5] M. Duarte, C. Dick, and A. Sabharwal, "Experiment-driven characterization of full-duplex wireless systems of full-duplex wireless systems," *IEEE Transactions on Wireless Communications*, **17**, 12, December 2012, pp. 4296–4307, doi: 10.1109/TWC.2012.102612.111278.
- [6] W. Cheng, X. Zhang and H. Zhang, "Heterogeneous statistical QoS provisioning over 5G wireless full-duplex networks," *2015 IEEE Conference on Computer Communications (INFOCOM)*, Hong Kong, April 2010, doi:10.1109/INFOCOM.2015.7218367.
- [7] L. Laughlin, M. A. Beach, K. A. Morris, and J. L.Haine, "Electrical balance duplexing for small form factor realization of in-band full duplex," *IEEE Communications Magazine*, **53**, 5, May 2012, pp. 102–110, doi: 10.1109/MCOM.2015.7105648.
- [8] N. Phungamngern, P. Uthansakul, and M. Uthansakul, "Digital and RF interference cancellation for single channel full-duplex transceiver using a single antenna," *10th International Conference on Electrical Engineering/Electronics, Computer, Telecommunications and Information Technology*, Krabi, Thailand, July 2013, doi: 10.1109/ECTICon.2013.6559508.